An asymptotically consistent approximant method with application to soft- and hard-sphere fluids

N. S. Barlow, A. J. Schultz, S. J. Weinstein, and D. A. Kofke

Citation: J. Chem. Phys. **137**, 204102 (2012); doi: 10.1063/1.4767065
View online: http://dx.doi.org/10.1063/1.4767065
View Table of Contents: http://jcp.aip.org/resource/1/JCPSA6/v137/i20
Published by the American Institute of Physics.

An asymptotically consistent approximant method with application to soft- and hard-sphere fluids

N. S. Barlow,[1,a)] A. J. Schultz,[1,b)] S. J. Weinstein,[2,c)] and D. A. Kofke[1,d)]
[1]*Department of Chemical and Biological Engineering, University at Buffalo, The State University of New York, Buffalo, New York 14260, USA*
[2]*Department of Chemical and Biomedical Engineering, Rochester Institute of Technology, Rochester, New York 14623, USA*

(Received 3 August 2012; accepted 29 October 2012; published online 26 November 2012)

A modified Padé approximant is used to construct an equation of state, which has the same large-density asymptotic behavior as the model fluid being described, while still retaining the low-density behavior of the virial equation of state (virial series). Within this framework, all sequences of rational functions that are analytic in the physical domain converge to the correct behavior at the same rate, eliminating the ambiguity of choosing the correct form of Padé approximant. The method is applied to fluids composed of "soft" spherical particles with separation distance r interacting through an inverse-power pair potential, $\phi = \epsilon(\sigma/r)^n$, where ϵ and σ are model parameters and n is the "hardness" of the spheres. For $n < 9$, the approximants provide a significant improvement over the 8-term virial series, when compared against molecular simulation data. For $n \geq 9$, both the approximants and the 8-term virial series give an accurate description of the fluid behavior, when compared with simulation data. When taking the limit as $n \to \infty$, an equation of state for hard spheres is obtained, which is closer to simulation data than the 10-term virial series for hard spheres, and is comparable in accuracy to other recently proposed equations of state. By applying a least square fit to the approximants, we obtain a general and accurate soft-sphere equation of state as a function of n, valid over the full range of density in the fluid phase. © *2012 American Institute of Physics*. [http://dx.doi.org/10.1063/1.4767065]

I. INTRODUCTION

The virial equation of state (VEOS, virial series) describes the dependence of pressure on density via a series expansion about the ideal-gas limit,[1] and is given by

$$Z \equiv \frac{P}{\rho \mathrm{k} T} = \underbrace{1 + \sum_{j=2}^{J} B_j \rho^{j-1}}_{\mathrm{VEOSJ}}, \tag{1}$$

where Z is the compressibility factor, P is the pressure, ρ is the number density, k is the Boltzmann constant, and T is the absolute temperature. The virial coefficients B_j are functions of T and the physical parameters describing the intermolecular potential. Specifically, the jth coefficient is given in terms of integrals over the positions of j molecules.[2] B_3, for example, requires integration over the variables describing the second and third molecules' positions relative to the first molecule. For illustration, the first two coefficients are written

$$B_2 = -\frac{1}{2V} \iint f_{12} d\mathbf{r}_1 d\mathbf{r}_2,$$
$$B_3 = -\frac{1}{3V} \iiint f_{12} f_{13} f_{23} d\mathbf{r}_1 d\mathbf{r}_2 d\mathbf{r}_3, \tag{2}$$

where f_{ab} is the Mayer f-function, $f_{ab} = [\exp(-\phi_{ab}/\mathrm{k}T) - 1]$, and ϕ_{ab} is the intermolecular potential between molecule a and molecule b with separation distance $r_{ab} = |\mathbf{r}_a - \mathbf{r}_b|$. Here, we examine the classical pair-wise additive and spherically symmetric repulsive soft-sphere potential, defined by

$$\phi_{ab} = \epsilon(\sigma/r_{ab})^n, \tag{3}$$

where ϵ, σ, and n are positive parameters, which characterize the energy, size, and "hardness" of the spheres, respectively. Note that when $n \to \infty$, Eq. (3) becomes the hard-sphere potential, and σ is interpreted in this limit as the hard-sphere diameter.

Standard quadrature methods are ineffective in calculating the multidimensional integrals that connect the virial coefficients to molecular interactions. Each increment in the order of the virial coefficient introduces integration over additional spatial variables for description of the new molecule's relative position, as well as (for non-spherical molecules) any other variables required to describe orientational and internal degrees of freedom. Moreover, the number of integrals involved in calculating virial coefficients increases rapidly and non-linearly with the order j of the coefficient. For example, the calculation of B_7 and B_8 requires the evaluation of 171 and 2606 Ree-Hoover cluster integrals, respectively, where each cluster integral represents a collection of nested integrals.[3] The Mayer sampling Monte Carlo (MSMC) approach is an effective way to compute these integrals, using importance

a)Electronic mail: barlow.nate@gmail.com.
b)Electronic mail: ajs42@buffalo.edu.
c)Electronic mail: sjweme@rit.edu.
d)Electronic mail: kofke@buffalo.edu.

sampling.[4] Still, for most simple molecular models, only the first 8 virial coefficients in Eq. (1) can be computed using the existing computational tools and methods, such as MSMC. If the virial series has poor convergence for the model being examined, an 8-term expansion (i.e., VEOS8) may give an inaccurate description of the fluid behavior. This is especially true if the system being examined has a large density range of physical interest, in which case a power series such as Eq. (1) will often incorrectly represent the entire range; the large-ρ behavior will be dominated by Jth term in the truncated series VEOSJ, and in most cases this asymptotic behavior is incorrect. This is expected, as the virial expansion is a Taylor series expanded around $\rho = 0$ and, provided enough terms are retained, is guaranteed to accurately represent the function $Z(\rho)$ only within its radius of convergence. This radius is determined by the distance to the singularity in $Z(\rho)$ nearest to $\rho = 0$ in the complex plane.

Over the last half-century, an effort has been made to remedy these issues by constructing equations of state using *approximants*, functions whose Taylor expansions about $\rho = 0$ match VEOSJ to order ρ^{J-1}. A review of various approximant types is given in Chisholm.[5] If the virial series has an inherent radius of convergence, an approximant can be used to analytically continue the series beyond this radius.[6] There are, however, an infinite number of analytic continuations that one can prescribe to a truncated series, through an infinite variety of approximants. Consequently, choosing the correct approximant that represents the equation of state is often nontrivial. Therefore, it is useful to have, in supplement with the virial series, additional information about the $Z(\rho)$ behavior for the model being described. This allows one to choose an appropriate class of approximants that correctly analytically continue the virial series. In this work, we introduce a method for constructing multi-point approximants that accurately match the $\rho \to 0$ and large ρ behavior of soft-sphere fluids, allowing us to form a general and accurate equation of state as a function of n, valid over the full range of ρ in the fluid phase. Additionally, this method leads to a fluid-phase equation of state for hard-spheres that is more accurate than the 10th order virial series, and is comparable in accuracy to other recent equations of state.

The paper is organized as follows. In Sec. II, convergence properties of the soft-sphere virial series are deduced and we examine the inability of the virial series to capture the large ρ behavior through a comparison with molecular simulation data. This motivates the formulation of asymptotically consistent approximants, described in Sec. III A, which are applied to the soft-sphere virial series. The approximant method is then extended to hard-spheres in Sec. III B, and a general equation of state (for any hardness n) is constructed in Sec. III C. In Sec. III D, we discuss the significance of branch points, as they relate to the radius of convergence of the virial series.

II. CONVERGENCE OF THE SOFT-SPHERE VIRIAL SERIES

The soft-sphere model, with a potential given by Eq. (3), has only one effective parameter, $\epsilon\sigma^n$. As a consequence, each virial coefficient can be evaluated at any temperature, through the relation $B_j = \bar{B}_j[\sigma^3(\frac{\epsilon}{kT})^{3/n}]^{j-1}$, provided the reduced virial coefficient $\bar{B}_j$ is known. Note, that in its reduced form, $\bar{B}_j$ is a function only of n, as can be deduced by writing the integral expressions (such as Eq. (2)) for $\bar{B}_j$ and then making the appropriate integration variable substitutions. $\bar{B}_2$ through $\bar{B}_8$ are given in Table I for various n values. $\bar{B}_2 = (2\pi/3)\Gamma(1 - 3/n)$ for soft-spheres and $\bar{B}_3$ is computed using fast Fourier transforms. Coefficients $\bar{B}_4$ through $\bar{B}_8$ in Table I are either taken from the literature,[7,8] or they are newly generated for this paper, computed using the MSMC method in the exact same manner as described in Tan *et al.*[8] For the "softer" potentials (small n) in Table I, the coefficients are relatively large and do not monotonically decrease with coefficient order. This leads to a poorly converging virial series, as emphasized by Wheatley.[7] In this section, we explore possible reasons for this poor convergence and its dependence on the hardness n. This analysis enables us to resolve convergence issues and develop a general equation of state that is accurate for all n, given in Sec. III C.

TABLE I. Reduced virial coefficients for the soft-sphere potential with hardness n. Numbers in parentheses give the 68% uncertainty in the final digit(s). Coefficients for $n = 6$, 9, and 12 are taken from Tan *et al.*[8] $\bar{B}_4$ and $\bar{B}_5$ for $n = 5$, 7, and 8 are taken from Wheatley.[7] $\bar{B}_4$ through $\bar{B}_6$ for $n = 24$, 50, and 80 are also taken from Wheatley.[7] All $\bar{B}$'s for hard-spheres ($n = \infty$) are taken from Clisby and McCoy,[9] which also reports $\bar{B}_9 = 0.4848(5)$ and $\bar{B}_{10} = 0.313(1)$. All other values are newly generated by the authors.

n	$\bar{B}_2$	$\bar{B}_3$	$\bar{B}_4$	$\bar{B}_5$	$\bar{B}_6$	$\bar{B}_7$	$\bar{B}_8$
4	7.5934596	9.05096	− 16.9058(9)	63.934(4)	− 325.87(8)	1993(3)	−10712(30)
5	4.645703	6.62922	− 2.18438	1.4702(1)	0.068(5)	− 5.93(8)	26.3(12)
6	3.712219	5.551999	1.44261(4)	− 1.68834(9)	1.8935(5)	− 1.700(3)	0.44(2)
7	3.264285	4.94326	2.70474	− 0.6886(1)	− 0.0888(10)	0.548(7)	− 0.9(1)
8	3.004449	4.55061	3.21509	0.3493(1)	− 0.4479(8)	0.228(5)	0.106(11)
9	2.836058	4.27563	3.43029(7)	1.08341(7)	− 0.21449(11)	− 0.0895(7)	0.071(4)
12	2.566507	3.79107	3.52761(6)	2.1149(2)	0.7695(2)	0.0908(5)	− 0.074(2)
24	2.282163	3.19804	3.18751	2.5338(1)	1.752(3)	1.09(2)	0.48(3)
50	2.174826	2.94499	2.90912	2.3801(1)	1.766(3)	1.14(9)	0.57(9)
80	2.142747	2.86546	2.80739	2.2926(1)	1.709(3)	1.30(2)	0.79(1)
200	2.11300	2.78986	2.7043(5)	2.189(2)	1.635(4)	1.196(18)	0.815(19)
∞	2.094395	2.74156	2.636218	2.121392(2)	1.56690(4)	1.09921(8)	0.7395(2)

We begin by examining the properties of the soft-sphere virial series for three representative cases: $n = 4$ (poor convergence), $n = 6$ (mild convergence), and $n = 12$ (good convergence). Convergence is ranked according to: (i) for a fixed ρ, the rate at which Z approaches a limiting value as more terms are added in the virial series; (ii) the extent of ρ over which such limiting values exist, allowing the series to converge. For soft-spheres, the virial series is currently (at most) given as an 8-term expansion. For a series with so few terms, standard convergence measures such as the root-test or ratio-test are not expected to provide reliable estimates for the radius of convergence.[9,10] As discussed later (Sec. III D), the radii of convergence of Taylor series of approximants to the virial series can be obtained explicitly; these hint at the dependence of the "actual" radius of convergence of the virial series on n (for small n).

Truncations of the virial series for $n = 4$, 6, and 12 are shown, respectively, in Figs. 1–3, where Z is plotted versus the reduced density $\bar{\rho} = \rho\sigma^3[\epsilon/(kT)]^{3/n}$. In the figures, the reduced freezing density, $\bar{\rho}_f$, is indicated, taken from Hoover *et al.*[12] ($n = 4$) and Tan *et al.*[8] ($n = 6$, 12). The fluid regime, defined as $0 \le \bar{\rho} \le \bar{\rho}_f$, is the range over which the virial series can (at best) be used to extract meaningful thermophysical properties. It is clear from Fig. 1(a) that VEOS8 gives a poor description of the $Z(\rho)$ behavior for $n = 4$. As the order of the virial series is increased for the $n = 4$ fluid, the series does in fact converge, but in a very small region near $\bar{\rho} = 0$, which is relatively far from $\bar{\rho}_f$. This can be seen in the magnification given in Fig. 1(b), where $Z(\rho)$ has been normalized by VEOS8. The region of convergence is larger for $n = 6$, as shown in Fig. 2. Still, for $n = 6$, the density at which VEOS7 deviates only 1% from VOES8 is far below freezing, as shown in the magnification (Fig. 2(b)). This is in contrast to the $n = 12$ virial series, shown in Fig. 3, where convergence of the series is visible over a large density range and $\bar{\rho}_f$ has a smaller magnitude, effectively making VEOS8 an accurate equation of state for the $n = 12$ soft-sphere fluid from low density to freezing. On the scale of Fig. 3(a), VEOS6, 7, and 8 are not distinguishable from the simulation data. As seen in the normalized Fig. 3(b) for $n = 12$, VEOS7 deviates (at most) 1% from the data and VEOS8 nearly matches the data to within its error bars.

We now continue to examine the convergence of the virial series for all n values given in Table I. To do this, we adopt the method used by Schultz and Kofke[13] and compute the "remainder sum" $r_m = \sum_{j=m+1}^{8} |\bar{B}_j|\bar{\rho}^j$ (note the absolute value)

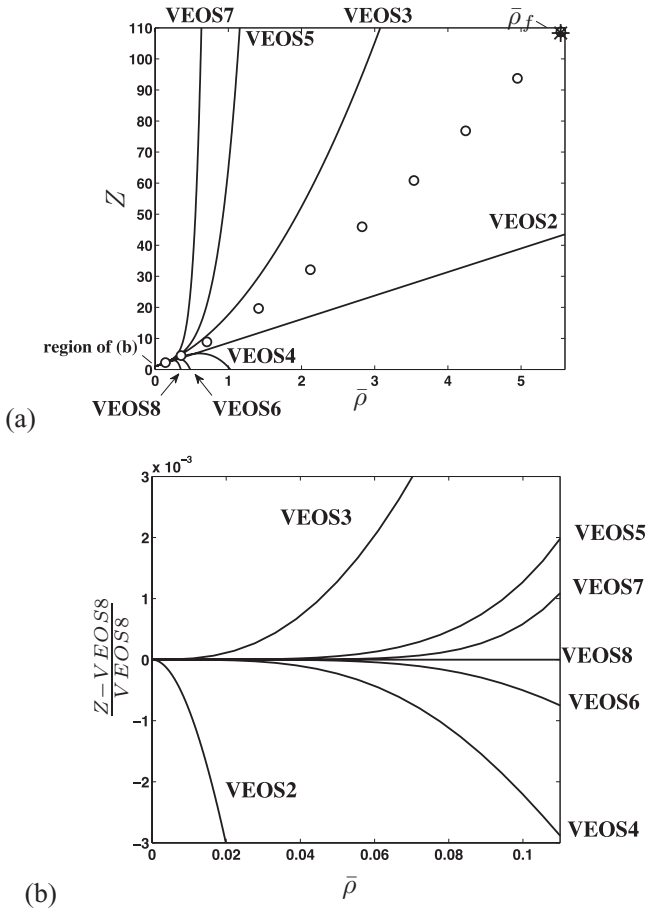

FIG. 1. Compressibility factor Z versus $\bar{\rho}$ for the $n = 4$ fluid, described by the truncated series VEOSJ ($J = 2 \ldots 8$). (a) Comparison with molecular simulation data[11] (○), given up to the freezing density $\bar{\rho}_f$ (✻). (b) Magnification of low-density region with Z normalized by VEOS8.

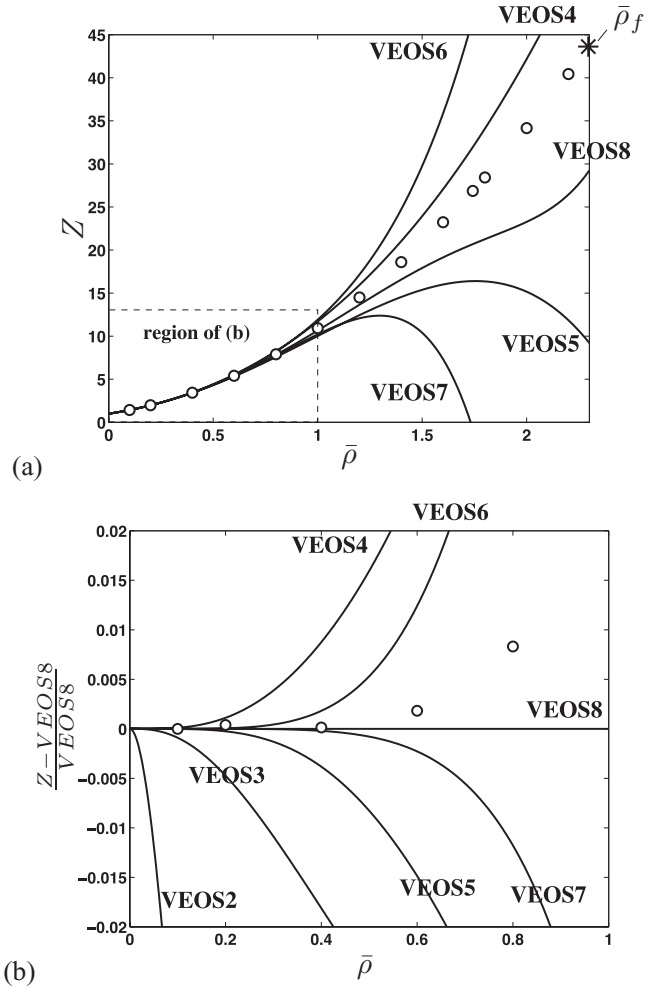

FIG. 2. Compressibility factor Z versus $\bar{\rho}$ for the $n = 6$ fluid, described by the truncated series VEOSJ ($J = 2 \ldots 8$). (a) Comparison with molecular simulation data[8] (○), given up to the freezing density $\bar{\rho}_f$ (✻). (b) Magnification of low-density region with Z normalized by VEOS8.

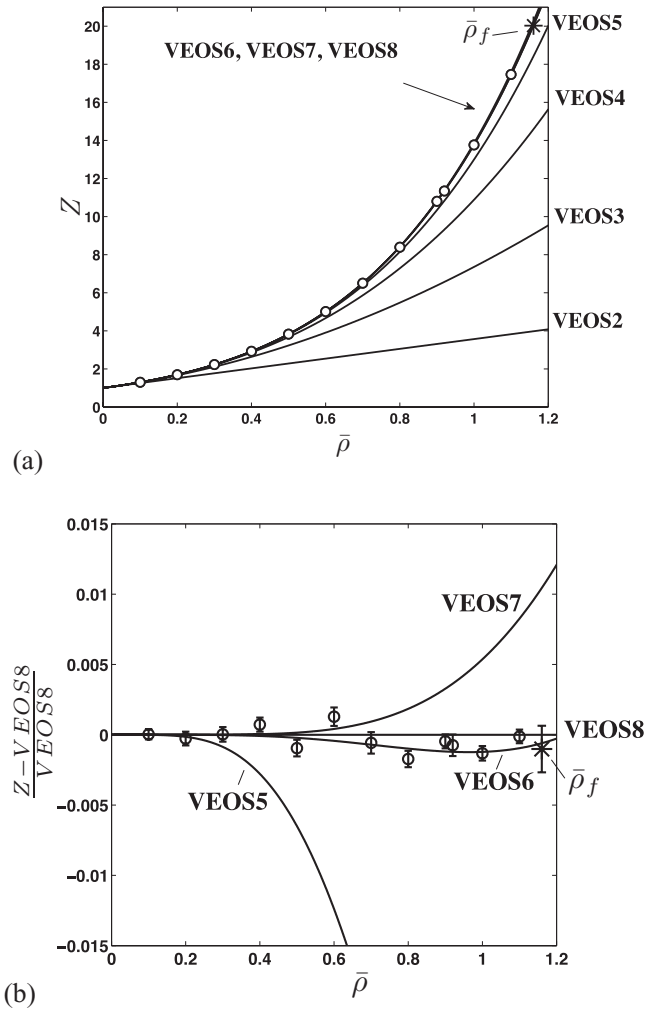

FIG. 3. Compressibility factor Z versus $\bar{\rho}$ for the $n = 12$ fluid, described by the truncated series VEOSJ ($J = 2 \ldots 8$). (a) Comparison with molecular simulation data[8] (○), given up to the freezing density $\bar{\rho}_f$ (✻). (b) Z normalized by VEOS8; uncertainty in the data is visible on this scale, shown by error bars.

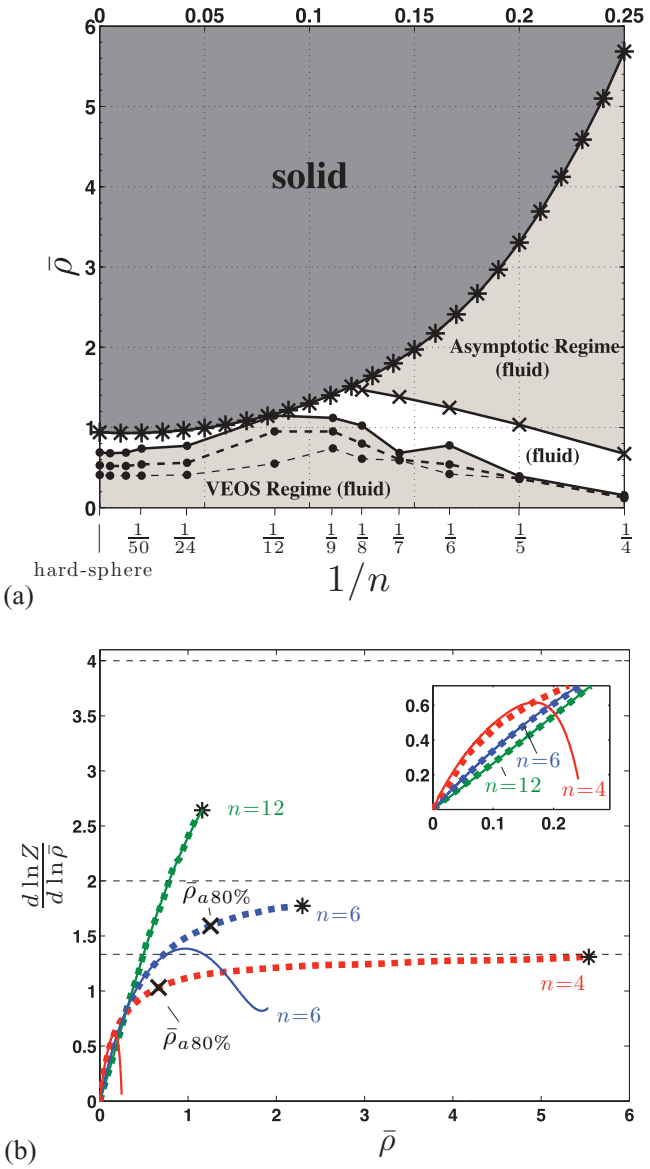

FIG. 4. (a) Reduced density $\bar{\rho}$ versus $1/n$. $\bar{\rho}_{1\%}$ curves ($-\bullet-$) indicate the densities at which the 4 term (lower curve), 5 term (middle curve), and 6 term (upper curve) remainder sums are less than 1% of the full sum. The $\bar{\rho}_f$ curve[14] ($-$✻$-$) places an upper limit on the region where the virial series is applicable. $\bar{\rho}_{a80\%}$ ($-\times-$) indicates where Z is within 80% of the asymptotic behavior (see (b)). (b) Fits through molecular simulation data (■■) and VEOS8 (—) are shown for $n = 4$, 6, and 12. Horizontal dashed lines indicate where the full $\frac{d\ln Z}{d\ln\bar{\rho}} = n/3$ asymptotic behavior is reached.

as well as the full sum $s = \sum_{j=1}^{8} |\bar{B}_j| \bar{\rho}^j$ (where $\bar{B}_1 = 1$). We then measure the density, $\bar{\rho}_{1\%}$, at which the remainder is less than 1%, expressed as a fraction of the full sum. By using the absolute value of coefficients, we are not measuring deviation from the true virial series; rather, we are measuring the contribution of adding terms to an analagous series. The absolute value here permits us to bypass the issue of coefficients changing sign, and allows us to make a fair comparison of convergence across different n values. The $\bar{\rho}_{1\%}$ values for $m = 4$, 5, and 6 are plotted versus $1/n$ in Fig. 4(a), along with the freezing densities $\bar{\rho}_f$, taken from Agrawal and Kofke.[14] Below, the $\bar{\rho}_f$ curve marks the fluid regime. In Fig. 4(a), notice that only the $n = 12$ case converges to within 1% over the full range of $\bar{\rho}$ in the fluid regime. For all other n values (especially, $n < 9$), $\bar{\rho}_f$ is larger than $\bar{\rho}_{1\%}$. In Fig. 4(a), the region below the uppermost ($m = 6$) $\bar{\rho}_{1\%}$ curve is labeled as the *VEOS regime*. Within this regime, VEOS8 can be considered an accurate equation of state, within a tolerance. On the other hand, the *asymptotic regime*, also shown in Fig. 4(a), defines a density range (for each $n < 9$) at which VEOS8 provides an inaccurate description of the fluid behavior; this is explained in the remaining portion of the section.

For large ρ, VEOSJ (given by Eq. (1)) behaves like $Z \sim \rho^{J-1}$. Interestingly, several semi-empirical and theoretical models[15–17] indicate that the correct large-ρ behavior for soft-spheres is $Z \sim \rho^{n/3}$. In order to determine the severity of this discrepancy when examining the physically relevant density range, we measure deviation between the "true" $Z(\rho)$ values (from molecular simulation) and the $\rho^{n/3}$ asymptotic behavior. In Fig. 4(a), the asymptotic regime is defined above the curve $\bar{\rho}_{a80\%}$, which indicates densities where the molecular simulation data are within 80% of the asymptotic behavior. The values along this curve are determined in the following

way. If the asymptotic behavior is given by $Z \sim \rho^{n/3}$, it follows that $\frac{d \ln Z}{d \ln \bar{\rho}} = n/3$. In Fig. 4(b), $\frac{d \ln Z}{d \ln \bar{\rho}}$ is plotted versus $\bar{\rho}$, and the asymptotic behavior for the $n = 4$, 6, and 12 fluids is given by the horizontal lines $\frac{d \ln Z}{d \ln \bar{\rho}} = 4/3$, 6/3, and 12/3. Fits through the simulation data and VEOS8 for $n = 4$, 6, and 12 are also shown in Fig. 4(b). The freezing density, which is also the last point of the simulation data, is indicated by a ✻. For $n = 4$ and $n = 6$, the data clearly approach the asymptotic behavior, more so for $n = 4$. The value $\bar{\rho}_{80\%}$ is indicated in Fig. 4(b) for $n = 4$ and 6. For $n = 12$ (and greater, not shown), the data never come within 80% of the asymptotic behavior. We shall now discuss the implications of this, with respect to the virial series.

In Fig. 4(a), it appears that, for $n \geq 12$, the VEOS regime encompasses most of the fluid regime, hence the virial series is expected to provide a reasonably accurate description of the correct thermodynamic behavior. As n becomes smaller ($n \leq 8$), the asymptotic behavior is approached near the freezing density. For $n \leq 6$, the asymptotic regime encompasses most of the fluid regime, and the virial series is not expected to represent the correct behavior, especially at high densities. This is because the virial series is a truncated power series, with asymptotic behavior (at large $\bar{\rho}$) given by the order of its truncation. The deficiency of using the virial series for high density and low n is remedied in Sec. III, where we provide a method for enforcing the correct asymptotic behavior for any truncation of the virial series.

III. ASYMPTOTICALLY CONSISTENT PADÉ APPROXIMANTS

As mentioned in Sec. I, the virial series can be approximately analytically continued beyond its radius of convergence by recasting the series as a judiciously chosen function that is analytic at $\rho = 0$. One of the most common types of analytic functions to use is the form of one polynomial in ρ divided by another polynomial in ρ; these are called Padé approximants. When the order of the numerator and denominator are the same, they are called symmetric Padés, and the large-ρ behavior is finite. For the physical systems studied by Baker and Gammel,[18] the true asymptotic behavior was finite, which precluded the use of the known truncated power-series when the independent variable (in our case, ρ) became large. The correct behavior was obtained by recasting each power series as a symmetric Padé. Here, we use a similar approach to that of Baker and Gammel,[18] except now to describe the soft-sphere system, we enforce a power-law asymptotic behavior.

A. Formulation

For the power series VEOSJ of order ρ^{J-1} given by Eq. (1), we construct $[(M+k)/(M-1-k)]^{\frac{\alpha}{2k+1}}$ or $[(M+k)/(M-k)]^{\frac{\alpha}{2k}}$ approximants of the form

$$Z = \left[\frac{\mathcal{N}_1 + \mathcal{N}_2\rho + \mathcal{N}_3\rho^2 + \cdots + \mathcal{N}_{M+k+1}\rho^{M+k}}{1 + D_2\rho + D_3\rho^2 + \cdots + D_{M-k}\rho^{M-1-k}}\right]^{\frac{\alpha}{2k+1}}, \quad J \text{ even}, M = J/2, \tag{4a}$$

or

$$Z = \left[\frac{\mathcal{N}_1 + \mathcal{N}_2\rho + \mathcal{N}_3\rho^2 + \cdots + \mathcal{N}_{M+k+1}\rho^{M+k}}{1 + D_2\rho + D_3\rho^2 + \cdots + D_{M-k}\rho^{M-k}}\right]^{\frac{\alpha}{2k}}, \quad J \text{ odd}, M = (J-1)/2, \tag{4b}$$

respectively, where $\mathcal{N}_1 = 1$, such that the ideal-gas limit $Z(0) = 1$ is recovered. M is a positive integer specifying the order of the approximant and k is an integer $\geq -M$ specifying the asymmetry between the numerator and denominator in Eq. (4). Note that symmetric Padés are not permissible with these definitions; a discussion is given later on the relevance of symmetric Padés to our problem. We choose $\alpha = n/3$ in Eq. (4) to match the asymptotic behavior for soft spheres, given by $Z \sim \rho^{n/3}$ for large ρ. The $\mathcal{N}$ and D coefficients are calculated algebraically, such that the Taylor expansion of Eq. (4) matches the virial series up to order ρ^{J-1}. Thus, Eq. (4) is an equation of state that matches both the $\rho \to 0$ and large-ρ behavior. In this sense, Eq. (4) is a type of multi-point Padé approximant, as classified by Chisholm.[5] Here, we shall refer to Eq. (4) specifically as an *asymptotically consistent approximant* (ACA). The standard Padé form is recovered by choosing $\alpha = 2k + 1$ (J even) or $\alpha = 2k$ (J odd) in the exponent of Eq. (4).

In Fig. 5, we show the various analytic continuations of the $n = 4$ virial series, using both standard and asymptotically consistent Padé approximants. For illustration, we choose to examine the $n = 4$ system because of its weakly converging virial series, shown in Sec. II (Fig. 1). It is clear from Fig. 5 that, as the order M increases, the ACAs coalesce into a curve that matches the simulation data. This is not the case for standard Padés, although they are significantly closer to the simulation data than VEOS8. The plot includes the asymmetric sequences of standard Padés, so that a direct comparison can be made with the ACAs. For example, when examining Fig. 5, one may track the Padé sequence ([1/0],[2/1],[3/2], [4/3]) or the asymptotically consistent sequence $([1/0]^{4/3}$, $[2/1]^{4/3}$, $[3/2]^{4/3}$, $[4/3]^{4/3})$ or the sequence of virial series, etc. If convergence can be established for a given sequence in the density range of physical relevance, the approximant is useful; the more rapid the convergence, the more useful the approximant is for providing the limiting (true) behavior.

TABLE II. Compressibility factor $Z(\bar{\rho})$ for various soft-sphere fluids, evaluated using Eq. (4a) with $\alpha = 2k + 1$ (standard Padés, left) and $\alpha = n/3$ (ACAs, right). ⋆ indicates a defective approximant. Note that the diagonal boldface entries (left) are virial series (VEOSJ), denoted by the $[(J-1)/0]$ Padés. For comparison, molecular simulation data[8,12] are given, with uncertainty reported in the final digits.

	Standard $[(M+k)/(M-1-k)]$ Padé approximants				Asymptotically consistent $\left[(M+k)/(M-1-k)\right]^{\frac{n/3}{2k+1}}$ approximants			
	$k=0$	$k=1$	$k=2$	$k=3$	$k=0$	$k=1$	$k=2$	$k=3$
KEY:								
M								
1	**[1/0]**				$[1/0]^{n/3}$			
2	[2/1]	**[3/0]**			$[2/1]^{n/3}$	$[3/0]^{n/9}$		
3	[3/2]	[4/1]	**[5/0]**		$[3/2]^{n/3}$	$[4/1]^{n/9}$	$[5/0]^{n/15}$	
4	[4/3]	[5/2]	[6/1]	**[7/0]**	$[4/3]^{n/3}$	$[5/2]^{n/9}$	$[6/1]^{n/15}$	$[7/0]^{n/21}$
$n=4$, $Z(5.5)$:								
M								
1	**42.764**				102.9633			
2	67.051	**-2.5×10^3**			108.1189	107.9112		
3	81.4085	−481.112	**-1.58×10^6**		108.1416	108.1047	108.0333	
4	78.1775	-9.496×10^2	2.211×10^5	**-1.58×10^9**	108.1362	108.1033	108.0305	109.0709
					Molecular simulation:[12] 108.67(5)			
$n=6$, $Z(2.2)$:								
M								
1	**9.1669**				25.8414			
2	⋆	**51.3995**			42.3645	37.7738		
3	39.9997	39.9929	**109.4331**		40.052	40.5162	39.3053	
4	40.6138	40.6075	−13.381	**26.439**	40.4133	40.3738	40.4288	39.8449
					Molecular simulation:[8] 40.43 (1)			
$n=12$, $Z(1.1)$:								
M								
1	**3.8232**				8.4665			
2	⋆	**13.1056**			18.8214	15.4233		
3	15.4937	⋆	**17.441**		17.473	⋆	16.669	
4	⋆	17.296	17.526	**17.458**	17.5033	17.161	⋆	17.112
					Molecular simulation:[8] 17.456(8)			

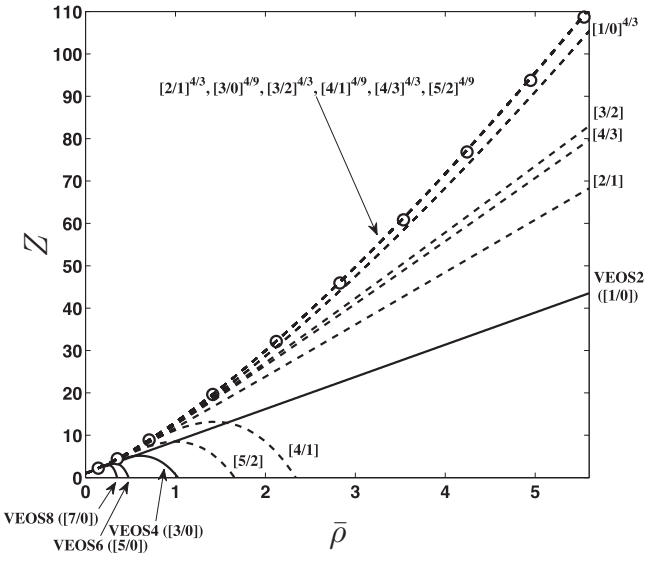

FIG. 5. Compressibility factor Z versus $\bar{\rho}$ for the $n=4$ fluid. The plot shows analytic continuations (- -) of the truncated series VEOSJ (—), given by standard $[(M+k)/(M-1-k)]$ Padé approximants and asymptotically consistent $\left[(M+k)/(M-1-k)\right]^{\frac{n/3}{2k+1}}$ approximants defined by Eq. (4); these are compared against molecular simulation data (○) from Rogers and Young.[11]

The convergence of the various approximants can perhaps be seen more clearly by choosing a specific density, fixing k in Eq. (4), and examining $Z(\bar{\rho})$ for increasing approximant order, M. In Table II, we examine the convergence in this manner for $n = 4$, 6, and 12 at $Z(\bar{\rho})$ close to freezing, where the virial series deviates the farthest from simulation data (see Fig. 4). For each n value in Table II, two sub-tables are given, one for standard Pade's (left) and the other for ACAs (right). Predictions from VEOS2, 4, 6, and 8 for the given density value are shown diagonally in boldface from top-left to bottom-right in the table of standard Padés. Approximant sequences of increasing order can be identified by increasing M, either vertically or diagonally in each sub-table, as indicated in the key at the top of Table II. Note, that reciprocal forms of the approximants (not shown in Table II) are unique for standard Padés (e.g., $[4/3] \neq [3/4]$), but not for ACAs (e.g., $[4/3]^{4/3} = [3/4]^{-4/3}$). When applied to the soft-sphere virial series, unique reciprocal Padé forms share the same poor convergence properties of the standard Padés shown in Table II. Padés and ACAs that have non-finite behavior in the physical domain (e.g., positive real poles) are considered defective, and are indicated by a ⋆ in the table.

When examining the $n = 4$ case in Table II, one can see a dramatic contrast between the convergence of ACA sequences and the lack of convergence in the standard Padé sequences. Here, the ACA sequences appear to converge to ~108, while the Padé sequences do not appear to converge at all. For comparison, Hoover *et al.*[12] report a value of $Z(5.5) = 108.67$ (5% uncertainty) from Monte Carlo molecular simulations of the $n = 4$ fluid.

When examining the $n = 6$ case in Table II, it is clear that the virial series does not converge for $\bar{\rho} = 2.2$, which we also observed in Fig. 2 (Sec. II). Here, the Padé sequences in the first two columns appear to converge to $Z(2.2) \approx 40.6$, while the Padés in the last two columns have wildly different values. This inconsistency of Padés for the $n = 6$ system was observed by Tan *et al.*;[8] they suggested using the [5/2] and [4/3] Padés ($M = 4$, $k = 1$ and 0). The ACAs resolve this issue, as all approximants converge to similar values. For comparison, Tan *et al.*[8] report a value of $Z(2.2) = 40.43$ (1% uncertainty) from Monte Carlo molecular simulations of the $n = 6$ fluid.

For the $n = 12$ system (Table II, bottom), both the virial series and the ACAs converge to similar Z values for $\bar{\rho} = 1.1$. This is also true for the standard Padés shown in the table. For comparison, Tan *et al.*[8] report a value of $Z(1.1) = 17.456$ (0.8% uncertainty) from Monte Carlo molecular simulations of the $n = 12$ fluid.

We now discuss the implications of using ACAs. The convergence properties of standard Padé sequences are such that the accuracy is expected to increase as $M \to \infty$, with k held fixed.[19] Like the partial sums of the virial series, a Padé sequence is a type of Cauchy sequence which, in this work, is required to limit to Z for a fixed ρ in order for the sequence to be useful. However, unlike the virial series, which may have a finite radius of convergence, Padé approximants to the virial series are expected to converge for the full range of ρ in the fluid regime. Padés are especially useful if the Padé sequence approaches its limiting behavior much faster than the partial sum sequence of the virial series. To obtain optimal convergence acceleration, Baker and Gammel[18] suggest constructing Padés that have the same asymptotic (in our case, large ρ) behavior as the physical system under study. For example, the symmetric Padé sequence is [1/1], [2/2], [3/3], etc. Since symmetric Padés are guaranteed to have finite (ρ^0) asymptotic behavior, one would expect decent convergence acceleration as $M \to \infty$ for physical systems with finite asymptotic behavior. Following Baker and Gammel,[18] this convergence acceleration is anticipated to hold for approximants defined by Eq. (4) for physical systems with power-law asymptotic behavior. It is clear from Table II that, when including more terms in the soft-sphere VEOS ($n = 4$, 6), the ACA sequences approach a limiting value, while the standard Padé sequences do not. Note, that if the asymptotic behavior is not approached within the fluid regime (e.g., $n = 12$, Fig. 4), any well-behaved approximant should suffice. In this case, however, the virial series will be accurate as well (Fig. 3, Table II), eliminating the need to compute approximants.

Table II indicates that, for a given order M, all variations in asymmetry k of the ACA lead to the same behavior, within a reasonable tolerance; we verified this over the full range of n. ACAs are designed such that this tolerance becomes small as ρ increases. Hence, $[7/0]^{n/21}$ ($k = 3$) appears to be as reasonable as any other ACA (i.e., any k) used to analytically continue VEOS8, where $M = 4$. The advantage of using $[7/0]^{n/21}$ is that the absence of a denominator precludes the existence of poles or negative-power branch points in the approximant. It should be mentioned that, for the soft-sphere cases studied here, complex and negative real poles or branch points are present in the ACAs that *do* have denominators. However, using $[7/0]^{n/21}$ allows us to demonstrate that the benefit of ACAs is *not* due to the allowance of poles or negative-power branch points in the function. In Table III, we make comparisons between the $[7/0]^{n/21}$ ACA, VEOS8, and simulation data for $n = 4$, 5, 6, 7, 8, 9, 24, 50, 80, and 200. As expected from Fig. 4 (Sec. II) and seen in Table III, the ACAs provide significant improvement over VEOS8 for $n < 9$ over the full range of densities. For $n \geq 9$, both the approximants and VEOS8 match the simulation data well. Before continuing, it should be noted that, even in the absence of $\bar{\rho}$ singularities that cause $Z(\bar{\rho}) = \infty$, $[7/0]^{n/21}$ approximants do have branch point singularities if $n/21$ is not an integer. The significance of branch points is discussed in Sec. III D.

In order to make a clear connection between the soft-spheres and the hard-sphere ($n = \infty$) limiting case, we define $N_j = \frac{n/3}{J-1}\mathcal{N}_{j>1}$ in Eq. (4) and write the $[(J-1)/0]^{(n/3)/(J-1)}$ approximant as

$$Z = \left\{1 + \frac{J-1}{n/3}[N_2\bar{\rho} + N_3\bar{\rho}^2 + \cdots + N_J\bar{\rho}^{J-1}]\right\}^{(n/3)/(J-1)}, \tag{5}$$

allowing us to take advantage of the identity $\lim_{m\to\infty}(1 + x/m)^m = e^x$. Letting $x = N_2\bar{\rho} + N_3\bar{\rho}^2 + \cdots + N_J\bar{\rho}^{J-1}$, $m = (n/3)/(J-1)$, and applying the exponential identity to Eq. (5) leads to an exponential approximant $[(J-1)/0]^{\infty}$ for hard-spheres,

$$\lim_{n\to\infty} Z(\rho, n) = \exp(N_2\bar{\rho} + N_3\bar{\rho}^2 + \cdots + N_J\bar{\rho}^{J-1}). \tag{6}$$

The N_j coefficients are found in the usual way, by equating like terms of the virial series with the Taylor expansion of Eq. (5) or Eq. (6). This leads to a linear system, which can be solved recursively; the solution is given in the Appendix for coefficients up to N_{10}. Note, that, unlike Eq. (5), the N_j coefficients of Eq. (6) are independent of truncation (i.e., $[2/0]^{\infty} = [1/0]^{\infty} + N_3\bar{\rho}^2$, $[3/0]^{\infty} = [2/0]^{\infty} + N_4\bar{\rho}^3$, etc). This feature can be seen in the recurrence solution (Appendix), letting $n \to \infty$. Briano and Glandt[20] performed a comprehensive study of all virial-like series that could be written to relate the pressure, density, and activity, combined in pairs. They considered both standard power series, as well as series written as the argument of an exponential function, such as Eq. (6). They observed that the exponential form of the pressure-versus-density series (i.e., Eq. (6)) performs significantly better than the standard virial series when applied to hard spheres. Note that Eq. (6) is a DLog Padé approximant[5] to the virial series, as it can be obtained by constructing the $[(J-1)/0]$ Padé of $d(\ln Z)/d\bar{\rho}$. We examine Eq. (6) in further detail in Sec. III B.

The N_j coefficients of the $[7/0]^{n/21}$ approximant are given in Table IV, and are computed using VEOS8 for soft-spheres.

TABLE III. Compressibility factor (Z) for soft-sphere fluids from molecular simulations, VEOS8, and $[7/0]^{n/21}$ using Eq. (4). Molecular simulation data for $n = 4$ are taken from Rogers and Young[11] (uncertainty not reported) and Hoover *et al.*[12] (for $\bar{\rho} = 5.5$). Molecular simulation data for $n = 6$, 9, and 12 are taken from Tan *et al.*[8] For other n values, simulations are done using 10^8 Monte Carlo steps and values reported are either for a system of 2048 atoms ($n \geq 24$), or for an infinite system extrapolated from simulations with 500 and 2048 atoms ($n \leq 8$). Numbers in parentheses give the uncertainty in the final digit(s).

n	$\bar{\rho}$	MC	VEOS8	$[7/0]^{n/21}$	n	$\bar{\rho}$	MC	VEOS8	$[7/0]^{n/21}$
4	0.14	2.225	2.205	2.564	9	0.1	1.329(3)	1.3299	1.3301
4	1.4	19.64	-9.94×10^4	19.53	9	0.5	3.973(1)	3.9759	3.9655
4	2.8	45.947	-1.35×10^7	45.919	9	0.9	10.082(3)	10.087	9.9221
4	4.2	76.853	-2.36×10^8	76.998	9	1.2	18.14(1)	18.188	17.604
4	5.5	108.67(5)	-1.58×10^9	109.07	12	0.1	1.2983(5)	1.2983	1.2983
5	0.1	1.5278(1)	1.5288	1.5288	12	0.5	3.825(2)	3.829	3.8271
5	0.7	6.9794(2)	8.5843	6.9945	12	0.9	10.802(5)	10.807	10.707
5	1.3	15.6454(5)	154.32	15.66	12	1.1	17.456(8)	17.112	17.458
5	1.9	27.017(1)	2111.7	26.997	24	0.2	1.6131(5)	1.6145	1.6146
5	2.5	40.798(2)	14690	40.713	24	0.45	3.111(1)	3.1114	3.1123
5	3	53.9872(3)	53350	53.819	24	0.7	6.359(3)	6.319	6.3361
6	0.1	1.4280(2)	1.428	1.428	24	0.8	8.592(4)	8.4818	8.5252
6	0.8	7.902(2)	7.8372	7.8897	24	0.95	13.70(1)	13.284	13.433
6	1.6	23.236(2)	19.142	23.025	50	0.2	1.5804(7)	1.5805	1.5805
6	2.2	40.43(1)	26.439	39.845	50	0.45	2.9812(15)	2.9819	2.9823
7	0.1	1.3788(1)	1.3785	1.3785	50	0.7	6.085(4)	6.0123	6.0259
7	0.44	3.5990(3)	3.5975	3.5977	50	0.8	8.319(6)	8.0852	8.1247
7	0.78	7.6088(4)	7.522	7.5877	80	0.2	1.5698(7)	1.5699	1.5699
7	1.12	13.7641(8)	12.509	13.657	80	0.45	2.938(2)	2.9396	2.9404
7	1.46	22.331(2)	13.584	22.031	80	0.7	5.961(3)	5.9226	5.9511
7	1.7	29.9695(19)	3.4085	29.431	80	0.8	8.154(4)	7.991	8.0749
8	0.1	1.3493(1)	1.3492	1.3492	80	0.95	13.53(2)	12.726	13.056
8	0.4	3.1403(4)	3.1411	3.1403	200	0.2	1.560(1)	1.5599	1.5599
8	0.7	6.4665(5)	6.4799	6.4528	200	0.45	2.893(2)	2.8951	2.8963
8	1	11.844(1)	12.006	11.761	200	0.7	5.828(4)	5.7819	5.8285
8	1.3	19.758(4)	20.762	19.485	200	0.8	7.922(6)	7.7773	7.9247
8	1.5	26.681(3)	29.376	26.164					

The coefficients are shown to monotonically decrease with n, with the exception of N_8 for $n > 80$. This is in contrast with the virial coefficients given in Table I which, as Wheatley[7] pointed out, oscillate with n for low n. In Sec. III C, we take advantage of the monotonicity of the N_j coefficients and develop a general equation of state for soft-spheres (for any n). But first, the properties of the hard-sphere exponential approximant given by Eq. (6) are examined.

B. Exponential approximant hard-sphere equation of state

For hard-spheres, two additional virial coefficients are available[9] beyond those shown in Table IV , $\bar{B}_9$ and $\bar{B}_{10}$, and so it is worth extending the order of our approximant. As mentioned in Sec. III A, the exponential approximant given by Eq. (6) has the unique feature that, as higher order

TABLE IV. Coefficients of $[7/0]^{n/21}$ for various soft-sphere fluids, computed using Eq. (5) and the known virial coefficients (Table I). Numbers in parenthesis give the error of the final digit, propagated from errors reported in Table I.

n	N_2	N_3	N_4	N_5	N_6	N_7	N_8
4	7.59346	131.5798	1283.141	7601.975(4)	27350.57(14)	55315(4)	51410(90)
5	4.64570	41.1613	214.013	706.9003(1)	1494.635(5)	1907.1(1)	1196(2)
6	3.71222	22.7777	84.941	208.52268(9)	341.325(1)	355.979(7)	201.37(4)
8	3.00445	11.8848	30.0229	52.4377(1)	64.5983(9)	54.706(6)	28.90(3)
9	2.83606	9.6378	21.2879	33.08562(7)	37.0291(3)	29.317(1)	15.160(5)
12	2.56651	6.2612	10.2967	12.3773(2)	11.2482(4)	7.7502(8)	3.914(2)
24	2.28216	2.87252	2.5538	1.8187(1)	1.152(3)	0.58(2)	0.23(3)
80	2.14275	1.17239	0.38028	0.1766(1)	0.138(3)	0.15(2)	− 0.16(3)
200	2.11300	0.79187	0.09504	0.076(2)	0.103(5)	0.04(2)	− 0.04(4)
∞	2.094395	0.54831	− 0.04334	0.057531(2)	0.07500(4)	− 0.0144(1)	− 0.0032(2)

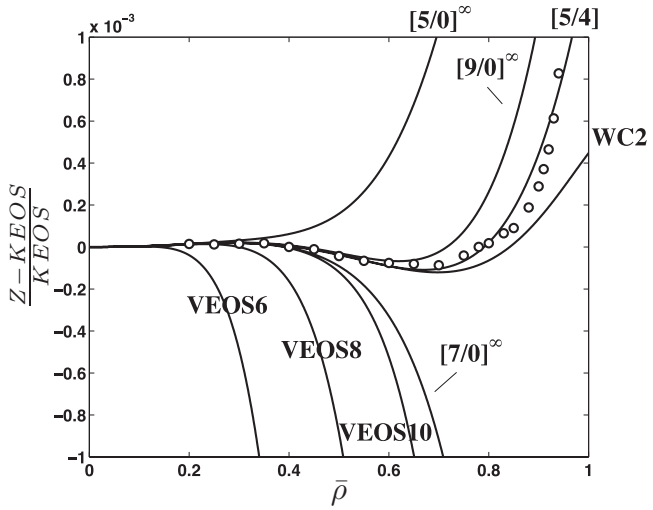

FIG. 6. Compressibility factor Z (for hard spheres) normalized by Kolafa's higher-order Carnahan-Starling-like equation[22] (KEOS) versus $\bar{\rho}$. The truncated series VEOSJ, asymptotically consistent (exponential) approximants $[(J-1)/0]^{\infty}$, the [5/4] Padé,[9] and the WC2 equation of state[23] (—) are compared against molecular simulation data[21] (○).

truncations of the virial series are used to construct the approximant and additional N_j coefficients arise, each lower-order N_j coefficient retains its numerical value, which is in contrast with the approximant given by Eq. (5) for finite n. The first 7 coefficients of Eq. (6) are given in the bottom row of Table IV (N_2 through N_8); additionally, $N_9 = 0.0168(7)$ and $N_{10} = -0.0018(15)$. A comparison between the exponential approximant $[9/0]^{\infty}$, VEOS10, and molecular simulation data from Kolafa *et al.*[21] is shown in Fig. 6, where the curves are normalized by a hard-sphere equation of state (KEOS) proposed by J. Kolafa, given in Boublík and Nezbeda.[22] KEOS is one order more accurate than the Carnahan-Starling equation, and is given by $Z = [1+\eta+\eta^2-\frac{2}{3}\eta^3(1+\eta)]/(1-\eta)^3$, where $\eta = \pi\bar{\rho}/6$. Normalization with a reasonably accurate equation of state, such as KEOS, enables us to visually distinguish between the exponential approximant and other highly accurate equations of state developed recently, namely the [5/4] Padé suggested by Clisby and McCoy[9] and the WC2 equation of state given by Bannerman *et al.*;[23] these are also shown in Fig. 6. Although not shown in the figure, we have also compared with equations of state given by Sanchez and Lee[24] and Tian *et al.*[25] All aforementioned equations provide significant improvement over VEOS10, and are comparable in accuracy to the $[9/0]^{\infty}$ approximant defined by Eq. (6).

Lower order approximants are also shown in Fig. 6, in order to illustrate the convergence of approximant sequences. As seen in the figure, the sequence $[5/0]^{\infty}$, $[7/0]^{\infty}$, $[9/0]^{\infty}$ converges to the simulation data faster than the sequence VEOS6, VEOS8, VEOS10. Convergence cannot be established for the $[M+1/M]$ Padé sequence containing [5/4], as all lower order Padés in this sequence are defective (have positive real poles). Note that the [5/4] Padé is the closest match to simulation data in Fig. 6. However, [5/4] is better thought of as a fit to the data, as convergence of the $[M+1/M]$ sequence does not allow one to deduce that [5/4] is, in fact, the "best" Padé approximant for $J = 10$, without making a comparison with molecular simulation data.

A virial coefficient prediction matrix is given in Table V, which lists the coefficients of Taylor expansions of $[(J-1)/0]^{\infty}$ approximants, given by Eq. (6). Coefficients beyond B_J are the "predicted" virial coefficients; they are a direct result of the analytic continuation imposed by the approximant, and have not been calculated via the molecular interaction models that define the actual virial coefficients. If we Taylor expand the exponential approximant $[9/0]^{\infty}$ to, say, 16 terms, we could obtain predictions for B_{11} through B_{16} for hard spheres. We do not list these here, but one can easily compute them (for any order) from Eq. (6). It is interesting to note that although a variety of different hard-sphere equations of state are used, similar values for these extrapolated virial coefficients are found in the literature.[9,23,25–27] B_{11} and B_{12}, shown here in Table V, also closely match the predictions of Guerrero and Bassi.[28] It has been conjectured[9,10] that the coefficients of the hard-sphere virial series may become negative at sufficiently large J. To address this interest, we note that, while the predicted virial coefficients extracted from Eq. (6) monotonically decrease with increasing order J, they do not become negative (at least not up to B_{16}). This is also seen in the aforementioned virial coefficient prediction literature. Although negative coefficients may occur for higher-order extrapolations (e.g., Bannerman *et al.*[23]), the margin of uncertainty here is large and such extrapolations are unsuitable for drawing conclusions on this issue.

TABLE V. Demonstration of the potential for $[(J-1)/0]^{\infty}$ approximants to predict hard sphere virial coefficients. For a given virial series of order J, including virial coefficients up to $\bar{B}_J$ (shown in bold, from Clisby and McCoy[9]), the "predicted" $\bar{B}_{j>J}$ coefficients from the Taylor expansion of Eq. (6) are listed horizontally. For a truly predictive approximant, each predicted $\bar{B}_j$ should limit to the actual virial coefficient as J increases. Numbers in parenthesis give the error of the final digit, propagated from errors reported in Table I.

J	$\bar{B}_4$	$\bar{B}_5$	$\bar{B}_6$	$\bar{B}_7$	$\bar{B}_8$	$\bar{B}_9$	$\bar{B}_{10}$	$\bar{B}_{11}$	$\bar{B}_{12}$
3	2.67955	2.15462	1.49022	0.91399	0.5069	0.2580	0.1218	0.0538	0.0224
4	**2.63622**	2.06386	1.37141	0.79880	0.4155	0.1960	0.0847	0.0338	0.0126
5		**2.12139**	1.49190	0.95653	0.5672	0.3164	0.1671	0.0843	0.0408
6			**1.56690(4)**	1.11361(1)	0.7728(1)	0.5141(1)	0.3262(1)	0.1990(1)	0.11847(4)
7				**1.09921(8)**	0.7426(2)	0.4746(3)	0.2882(2)	0.1685(2)	0.09591(15)
8					**0.7395(2)**	0.4680(4)	0.2795(6)	0.1601(6)	0.0892(5)
9						**0.4848(5)**	0.315(1)	0.2061(15)	0.1334(15)
10							**0.313(1)**	0.202(2)	0.128(3)

TABLE VI. Coefficients of fit equation, Eq. (7).

	$j=3$	4	5	6	7	8
C_1	37.68093	31.84336	12.88986	0.6244331	7.697069	−17.8162
C_2	−249.7449	−28.27901	351.9601	547.0779	290.0482	659.0062
C_3	1001.704	−143.4443	−2051.451	−2871.629	−998.4549	−3016.937
C_4	−995.2711	710.271	3476.869	4530.886	1376.421	4595.473
C_5	−642.922	401.1219	2043.935	2823.564	954.9595	3046.475
C_6	−249.4429	151.409	761.7278	1090.136	396.4693	1234.401
C_7	−79.73547	48.25811	238.9029	350.585	135.0571	413.1661
C_8	−23.60437	14.89787	69.17048	102.5482	41.64036	125.0602
C_9	−6.366601	4.362856	19.08495	28.573	12.55009	36.4512

As shown in each column of Table V, the predicted virial coefficients appear to limit to the actual virial coefficient (shown in bold) as J increases. Using VEOS6, the exponential approximant predicts B_7 through B_{10} within 2% − 6%. Recently, Ončák *et al.*[26] constructed hard-sphere equations of state, using both lower order virial coefficients (in the same fashion as an approximant) and simulation data. Using VEOS6, the approximants of Ončák *et al.*[26] predict B_7 through B_{10} within ≤2%. Also, using the aforementioned approximants, one is able to predict high-order coefficients to a higher of degree of accuracy and using fewer terms (e.g., VEOS4) than if one used the exponential approximants given here.

For any type of approximant, predictive capability is somewhat expected from the convergence properties discussed in Sec. III A. One should be cautious, however, in using predicted virial coefficients to generate higher-order approximants, as this does not incorporate any new data and is therefore not expected to improve the description of fluid behavior. We include Table V here only to demonstrate the self-consistency and robustness of the ACA method.

C. General soft-sphere equation of state

In Wheatley,[7] an "effective hard-sphere" formulation was applied to the soft-sphere model, where an expansion in effective hard-sphere diameter was substituted into the soft-sphere virial series for each hardness n. For $n \geq 10$, the effective hard-sphere diameter coefficients were observed to vary more smoothly with n than the virial coefficients, allowing Wheatley[7] to generate fits for the hard-sphere diameter coefficients as a function of n, leading to a general and accurate equation of state for $n \geq 10$; we refer to this here as WFIT. The $[7/0]^{n/21}$ approximants described in Sec. III A have coefficients (Table IV) that similarly vary more smoothly with n than the virial coefficients (Table I), but now over the full range of n. Using a least-squares method, we construct a general equation of state (for any ρ and n), given by Eq. (5) with coefficients defined by $N_2 = \bar{B}_2 = (2\pi/3)\Gamma(1-3/n)$ and

$$N_j(n) = \exp[C_1/n + C_2/n^2 \ldots C_9/n^9] - 1 + N_j(\infty), \quad j = 3 \ldots 8, \tag{7}$$

where C_1 through C_9 are given in Table VI and the $N_j(\infty)$'s are given in the bottom row of Table IV. We shall refer to this fitted general equation of state as asymptotically consistent approximant fit (ACAFIT), defined by Eq. (5), Eq. (7), and Table VI. By design, ACAFIT is exactly equal to Eq. (6) for $n = \infty$.

To test ACAFIT for n values not used in the fit, a comparison is made against molecular simulation data (from Table III) for $n = 7$ and $n = 50$ in Figs. 7(a) and 7(b), respectively. One can see from Fig. 7(a) that ACAFIT provides substantial improvement over VEOS8 for $n = 7$. WFIT is given in Fig. 7(a) for reference only; as Wheatley[7] points out, the fit is not constructed to do well for $n < 10$. For $n = 50$ (Fig. 7(b)), WFIT is a closer match to the simulation data than ACAFIT and VEOS8, although all equations of state do reasonably well.

Note that in our fit, we use VEOS8 to construct approximants for 5 different n values covering the range $4 \leq n < 10$ and 5 values covering the range $10 < n \leq \infty$. In comparison, Wheatley[7] used VEOS4 to construct effective hard-sphere equations for 19 different n values covering the range $10 \leq n \leq \infty$. While the asymptotic approximant method that we propose in Sec. III A stands on its own, the fit that we present in this section can always be improved by refining the set of hardness (n) values used and/or including higher order virial coefficients, as they become available through advances in computational methods and architecture.

In summary, if the virial coefficients and asymptotic behavior of $Z(\rho)$ are known and $n < 9$, we suggest trying an asymptotic approximant in place of the virial series; one may use the formula given in the Appendix to build the approximant. If the virial coefficients are not known and $4 < n < 10$, ACAFIT can be used as a reasonably accurate equation of state. If the virial coefficients are not known and $10 \leq n < \infty$, one may either use ACAFIT, or the effective hard-sphere fit given by Wheatley.[7] For $n \geq 12$, one may also consider forming accurate equations of state by using the analytic forms of $Z(\rho)$ given in Branka and Heyes.[30]

D. Branch points and radii of convergence of virial series

The radius of convergence of the virial series for $Z(\rho)$ limits its range of utility, and is thus a critical characteristic of the series. As the density approaches this radius from below, additional terms are required to construct the series if one wishes to retain accuracy. Practically, the number of virial series terms is limited by our ability to calculate

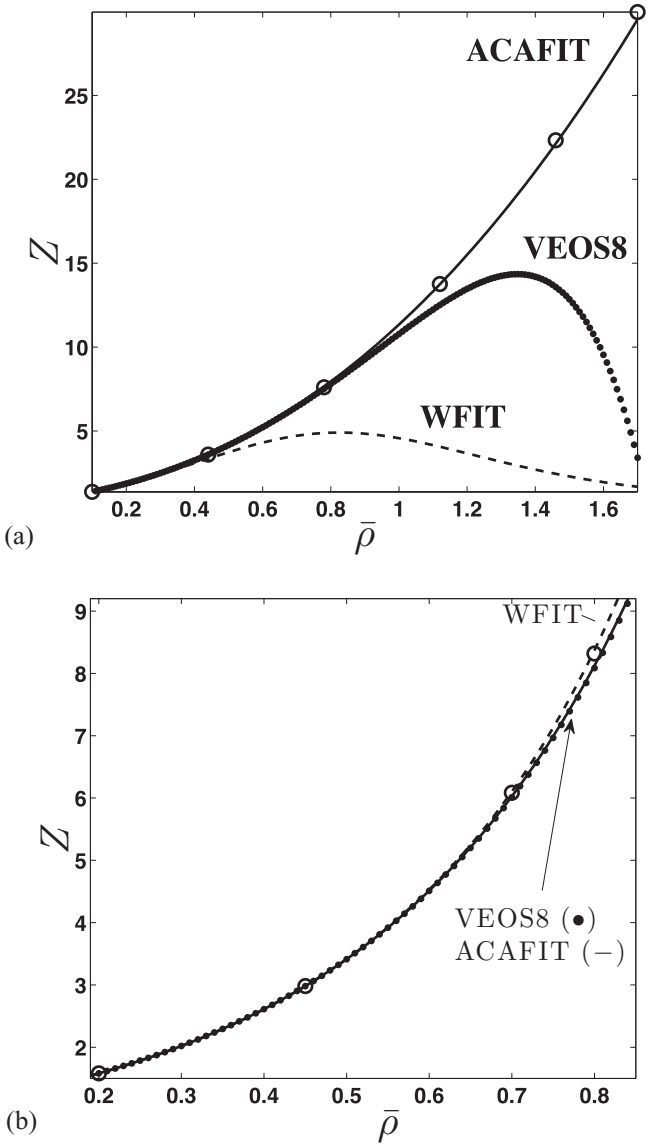

FIG. 7. Compressibility factor Z plotted versus $\bar{\rho}$ for the (a) $n = 7$ and (b) $n = 50$ soft-sphere fluids. In both figures, VEOS8 (•); the asymptotic approximant fit (ACAFIT, —) defined by Eq. (5), Eq. (7), and Table VI; and WFIT[7] (- -) are compared against molecular simulation data (○, Table III).

coefficients, and so even in regimes where the series should converge, the accuracy of a finite-term virial series can be lost even before one reaches this convergence radius. For densities larger than the radius of convergence, the truncated virial series expression for $Z(\rho)$ could be reasonably accurate. However, in this regime, the series will eventually diverge as more terms are added. Our ability to deduce these distinctions is lost with finite-term representations of infinite expansions, as the radius of convergence can never be precisely determined without knowing all terms of the virial series. Despite these limitations, it is instructive to consider the origin of the radius of convergence, implied by results of this study. It is well known that singularities in the function being represented (when examined in the complex plane) are the origin of a finite radius of convergence. Traditional finite-term Padé approximants assume that these singularities are in the form of poles. In the current study, the form given by Eq. (5) suggests

TABLE VII. Radii of convergence of Taylor expansions of $[(J-1)/0]^{(n/3)/(J-1)}$ approximants, given by the branch point of smallest magnitude. If $(n/3)/(J-1)$ is an integer, the approximant is a polynomial; these spaces are left blank. Numbers in parenthesis give the error of the final digit, propagated from errors reported in Table I.

J	$n=4$	5	6	7	8
2	0.1756	0.3588		0.7148	0.8876
3	0.1686	0.3079		0.5282	0.6242
4	0.1600	0.3017	0.4051	0.4968	0.5817
5	0.1475	0.2695	0.3716	0.4576	0.5341
6	0.1365	0.2598	0.3531	0.4314	0.5019
7	0.1319(3)	0.2498(2)	0.3399	0.4159(1)	0.4823(1)
8	0.1092(2)	0.2418(7)	0.3280(1)	0.4022(7)	0.4634(2)

that branch points, which are also singularities in the complex plane, could be the origin of a finite radius of convergence imposed on the virial series; this was suggested by Santos and de Haro[29] for hard-spheres. For our soft-sphere approximant given by Eq. (5) (ACA), branch points arise when $(n/3)/(J-1)$ is not an integer, and they are defined as ρ values, where the argument of the approximant is zero, thereby making derivatives of the approximant undefined (at some order). The virial series is, by definition, an expansion about $\rho = 0$; hence, the radius of convergence extracted from an ACA will be determined by the distance to the density closest to zero where a derivative of Eq. (5) is non-finite.

We first focus on very soft ($n \leq 8$) soft-sphere fluids, which clearly access the asymptotic regime shown in Fig. 4(a), and thus where we are confident that the $Z \sim \rho^{n/3}$ behavior is approached. The radii of convergence for expansions of the $[(J-1)/0]^{(n/3)/(J-1)}$ approximants are given in Table VII for $n \leq 8$. For a fixed order, J, the radii monotonically increase with n, which is consistent with convergence behavior in the VEOS regime of Fig. 4(a) (for $n \leq 8$). For a fixed n, the radii monotonically decrease with order J. The values of the radii in Table VII are all of the appropriate order of magnitude, where one might expect the virial series to diverge. Certainly, for densities less than the values given in Table VII, the virial series converges well (c.f., Fig. 4(a)). Radii of convergence given by branch points of other ACAs (not shown), of the general form given by Eq. (4), are close to those given in Table VII. In contrast, the poles of various Padés (not shown), when applied to the soft-sphere virial series for small n, impose radii of convergence that vary drastically at each order J. This is expected, as convergent sequences of Pade's cannot be constructed for small values of n, as shown in Sec. III A, and their predictive behavior is erratic. In summary, the success of asympotically consistent approximants over standard Padé approximants at forming convergent sequences of only 7-terms (see Sec. III A) suggests that, for small n ($n \leq 8$), the radius of convergence imposed on the virial series for (very soft) soft spheres is more likely determined by branch point singularities rather than isolated singularities such as poles.

For large n ($n \geq 9$), the asymptotic behavior is not approached in the fluid regime, and the virial series converges rather well (c.f., Fig. 4(a)). This suggests that the singularity

closest to $\rho = 0$ lies in the range of densities in which the fluid solidifies, rendering the radius of convergence irrelevant, practically.

IV. DISCUSSION AND CONCLUDING REMARKS

Asymptotically consistent approximants (ACAs) are well-suited for the soft-sphere model because the "large" ρ asymptotic behavior is, in fact, approached at relatively low densities, particularly for soft-sphere fluids with a low hardness ($n < 9$). When attempting to analytically continue the virial series for these fluids, standard Padé approximant sequences converge slowly, and no consistent limit (between sequences) is approached for the available 8-term series. This forces one to choose between different Padés, each describing drastically different thermodynamic behavior. Such a choice can be made only if molecular simulation data are available, in which case any chosen Padé is effectively a fit to the data. In the absence of simulation data, Padé approximants are thus rendered useless at predicting the behavior of soft-sphere fluids, particularly for $n < 9$. This is expected, since the integer power-law asymptotic behavior inherent to Padés is given by the difference in order between the numerator and denominator of the Padé. Since the asymptotic behavior is different for most Padé sequences that are constructed, it is impossible for all sequences to uniformly agree with the true large ρ behavior of the fluid.

The analysis provided in this work validates the use of ACAs as accurate equations of state for soft-sphere fluids. The proposed approximant is a simple extension of a two-point Padé, satisfying the zero-density expansion (virial series) of compressibility, $Z(\rho)$, as well as the large ρ asymptotic behavior; the method may be extended to other models, provided these behaviors are known. ACAs give one the freedom to explicitly prescribe an asymptotic behavior, and enable the construction of convergent sequences while holding the asymptotic behavior fixed. If convergence is achieved for all ACA sequences before exhausting all terms of a truncated power series (e.g., virial series), as is the case for soft-spheres, an approximant can be chosen from any sequence, and can be used as an accurate equation of state; this conclusion is validated through comparison with molecular simulation data.

Out of the possible ACA sequences, we suggest choosing the form with no denominator, so as to eliminate the possibility of non-finite $Z(\rho)$ behavior. Using this form, we take advantage of the monotonicity of the ACA coefficients with n, and construct a least-squares fit, which leads to an accurate soft-sphere equation of state for $Z(\rho, n)$, valid over the range $4 \leq n \leq \infty$ and for all densities in the fluid state. This general equation of state is validated against molecular simulation data, using values of n not included in the fit. For hard spheres ($n = \infty$), the ACA limits to an exponential equation of state, which is closer to simulation data than the 10-term virial series for hard spheres, and is comparable in accuracy to other recent equations of state. Although it is impossible to tell without obtaining significantly more terms (i.e., virial coefficients), the success of ACAs over Padés in describing the soft-sphere fluid behavior indicates that branch points, rather than poles, are likely responsible for the divergence of the virial series, for small n ($n \leq 8$).

The method provided here returns to the intentions of the seminal Padé paper by Baker and Gammel,[18] in that we are simply choosing an approximant that matches the asymptotic behavior. We recognize that soft-spheres are a unique case where the large-ρ behavior can be deduced as a simple power-law. However, perhaps the benefit of using ACAs to form accurate equations of state, shown here for soft-spheres, will motivate the development of techniques used to extract the asymptotic behavior of fluids described by more elaborate molecular potentials.

ACKNOWLEDGMENTS

This work is supported by the U.S. National Science Foundation (NSF) (Grant Nos. CHE-1027963 and CBET-0854340). N. S. Barlow is supported by the NSF award (Award No. CI-TraCS-1048579). Computational resources were provided by the University at Buffalo Center for Computational Research.

APPENDIX: RECURRENCE SOLUTION

Given VEOSJ, the coefficients of $[(J-1)/0]^{(n/3)/(J-1)}$ can be computed recursively. The first nine coefficients of Eq. (5) are given by

$$N_2 = \bar{B}_2, \quad N_3 = \bar{B}_3 - C_1 N_2^2,$$

$$N_4 = \bar{B}_4 - C_2 N_2^3 - 2C_1 N_3 N_2,$$

$$N_5 = \bar{B}_5 - C_3 N_2^4 - 3C_2 N_2^2 N_3 - 2C_1 N_4 N_2 - C_1 N_3^2,$$

$$N_6 = \bar{B}_6 - C_4 N_2^5 - 4C_3 N_2^3 N_3 - 3C_2 N_4 N_2^2 - 3C_2 N_2 N_3^2 - 2C_1 N_5 N_2 - 2C_1 N_4 N_3,$$

$$N_7 = \bar{B}_7 - C_5 N_2^6 - 5C_4 N_2^4 N_3 - 4C_3 N_2^3 N_4 - 6C_3 N_2^2 N_3^2 - 3C_2 N_5 N_2^2 - 6C_2 N_2 N_3 N_4 - 2C_1 N_6 N_2 - C_2 N_3^3 - 2C_1 N_5 N_3 - C_1 N_4^2,$$

$$N_8 = \bar{B}_8 - C_6N_2^7 - 6C_5N_2^5N_3 - 5C_4N_2^4N_4 - 10C_4N_2^3N_3^2 - 4C_3N_5N_2^3 - 12C_3N_2^2N_3N_4 - 3C_2N_6N_2^2$$
$$-4C_3N_2N_3^3 - 6C_2N_5N_2N_3 - 3C_2N_2N_4^2 - 2C_1N_7N_2 - 3C_2N_3^2N_4 - 2C_1N_6N_3 - 2C_1N_5N_4,$$
$$N_9 = \bar{B}_9 - C_7N_2^8 - 7C_6N_2^6N_3 - 6C_5N_2^5N_4 - 15C_5N_2^4N_3^2 - 5C_4N_2^4N_5 - 20C_4N_2^3N_3N_4 - 4C_3N_6N_2^3$$
$$-10C_4N_2^2N_3^3 - 12C_3N_2^2N_3N_5 - 6C_3N_2^2N_4^2 - 3C_2N_7N_2^2 - 12C_3N_2N_3^2N_4 - 6C_2N_6N_2N_3$$
$$-6C_2N_2N_4N_5 - 2C_1N_8N_2 - C_3N_3^4 - 3C_2N_3^2N_5 - 3C_2N_3N_4^2 - 2C_1N_7N_3 - 2C_1N_6N_4 - C_1N_5^2,$$
$$N_{10} = \bar{B}_{10} - C_8N_2^9 - 8C_7N_2^7N_3 - 7C_6N_2^6N_4 - 21C_6N_2^5N_3^2 - 6C_5N_2^5N_5 - 30C_5N_2^4N_3N_4 - 5C_4N_6N_2^4 - 20C_5N_2^3N_3^3$$
$$-20C_4N_2^3N_3N_5 - 10C_4N_2^3N_4^2 - 4C_3N_7N_2^3 - 30C_4N_2^2N_3^2N_4 - 12C_3N_6N_2^2N_3 - 12C_3N_2^2N_4N_5 - 3C_2N_8N_2^2$$
$$-5C_4N_2N_3^4 - 12C_3N_2N_3^2N_5 - 12C_3N_2N_3N_4^2 - 6C_2N_7N_2N_3 - 6C_2N_6N_2N_4 - 3C_2N_2N_5^2 - 2C_1N_9N_2$$
$$-4C_3N_3^3N_4 - 3C_2N_6N_3^2 - 6C_2N_3N_4N_5 - 2C_1N_8N_3 - C_2N_4^3 - 2C_1N_7N_4 - 2C_1N_6N_5,$$

where

$$C_Q = \prod_{q=1}^{Q} \frac{1 - q^{\frac{J-1}{n/3}}}{q+1}.$$

[1] E. A. Mason and T. H. Spurling, *The Virial Equation of State* (Pergamon, New York, 1969).
[2] D. A. McQuarrie, *Statistical Mechanics* (University Science Books, California, 1973).
[3] F. H. Ree and W. G. Hoover, J. Chem. Phys. **41**, 1635 (1964).
[4] J. K. Singh and D. A. Kofke, Phys. Rev. Lett. **92**, 220601 (2004).
[5] J. S. R. Chisholm, Circuits Syst. Signal Process. **1**, 279 (1982).
[6] G. A. Baker, *Quantitative Theory of Critical Phenomenon* (Academic, 1990), p. 228.
[7] R. J. Wheatley, J. Phys. Chem. B **109**, 7463 (2005).
[8] T. B. Tan, A. J. Schultz, and D. A. Kofke, Mol. Phys. **109**, 123 (2011).
[9] N. Clisby and B. M. McCoy, J. Stat. Phys. **122**, 15 (2006).
[10] D. S. Gaunt and G. S. Joyce, J. Phys. A **13**, L211 (1980).
[11] F. J. Rogers and D. A. Young, Phys. Rev. A **30**, 999 (1984).
[12] W. G. Hoover, S. G. Gray, and K. W. Johnson, J. Chem. Phys. **55**, 1128 (1971).
[13] A. J. Schultz and D. A. Kofke, Mol. Phys. **107**, 2309 (2009).
[14] R. Agrawal and D. A. Kofke, Mol. Phys. **85**, 23 (1995).
[15] D. M. Heyes, S. M. Clarke, and A. C. Brańka, J. Chem. Phys. **131**, 203505 (2009).
[16] Y. Rosenfeld and A. Baram, J. Chem. Phys. **75**, 427 (1981).
[17] Y. Song and E. A. Mason, Phys. Rev. A **44**, 8400 (1991).
[18] G. A. Baker and J. L. Gammel, J. Math. Anal. Appl. **2**, 21 (1961).
[19] C. M. Bender and S. A. Orszag, *Advanced Mathematical Methods for Scientists and Engineers I: Asymptotic Methods and Perturbation Theory* (McGraw-Hill, 1978), p. 388.
[20] J. G. Briano and E. D. Glandt, Fluid Phase Equilib. **5**, 207 (1981).
[21] J. Kolafa, S. Labík, and A. Malijevský, Phys. Chem. Chem. Phys. **6**, 2335 (2004).
[22] T. Boublík and I. Nezbeda, Collect. Czech. Chem. Commun. **51**, 2301 (1986).
[23] M. N. Bannerman, L. Lue, and L. V. Woodcock, J. Chem. Phys. **132**, 084507 (2010).
[24] I. C. Sanchez and J. S. Lee, J. Phys. Chem. B **113**, 15572 (2009).
[25] J. Tian, Y. Gui, and A. Mulero, J. Phys. Chem. B **114**, 13399 (2010).
[26] M. Ončák, A. Malijevský, J. Kolafa, and S. Labík, Condens. Matter Phys. **15**, 23004 (2012).
[27] J. Hu and Y. X. Yu, Phys. Chem. Chem. Phys. **11**, 9382 (2009).
[28] A. O. Guerrero and A. B. Bassi, J. Chem. Phys. **129**, 044509 (2008).
[29] A. Santos and M. L. de Haro, J. Chem. Phys. **130**, 214104 (2009).
[30] A. C. Branka and D. M. Heyes, Phys. Rev. E **74**, 031202 (2006).